The Pion Tetrahedron Fabric and Evolution Cosmology

Rami Rom$^{(a)}$

Abstract: According to the Standard Model (SM) the quantum vacuum is not empty. However, General Relativity (GR) and the SM do not describe the vacuum structure. We propose a valence quark-based theory of the quantum vacuum structure based on a pion tetrahedron fabric that fills space with varying density. We assume that the valence quarks and antiquarks, u , d , $\tilde{u}$, $\tilde{d}$ that form the vacuum pion tetrahedron fabric. Motion of particles made of quarks on the vacuum pion tetrahedron fabric is performed by quark exchange reactions by tunneling through a double well potential and motion of massless particles are performed by internal degrees of freedom motion of the pion tetrahedron fabric. Active Galactic Nuclei (AGN) systems may be Carnot engines working between cold black hole (BH) and hot accretion disc reservoirs. The AGN Carnot cycle may create and emit to space pion tetrahedrons, protons, electrons and photons in pulses by the AGN jets. An alternative explanation for the observed expansion of the Universe may be the creation and emission of pion tetrahedrons to space by the AGN jets that expands the Universe quantum vacuum pion tetrahedron fabric from inside like a balloon. Shakura and Sunyaev thin accretion disc analytic expressions are used for calculating the pion tetrahedron mass and the number of pion tetrahedrons emitted by an AGN Carnot engine in a cycle.

Keywords: Quantum vacuum, Pion tetrahedrons, Active Galactic Nuclei (AGN), Supermassive Black Holes (SMBH), Quasi-Periodic Eruptions (QPEs), Thin Accretion Discs, Superradiance and Carnot Engines.

(a) Email: romrami@gmail.com

1. The Quantum Vacuum Structure and the Valence Quarks

According to the standard model (SM), the mass of the elementary particles is due to the Higgs mechanism where a non-zero vacuum expectation value (VEV) spontaneously breaks the chiral symmetry of the otherwise massless particle solution of the Dirac Lagrangian. The SM assumes that the quantum vacuum is not empty but does not tell what is the structure of the vacuum that creates the non-zero VEV and the Mexican hat potential[1-5]. The internal structure and spin of the elementary particles will be studied by the EIC[6]. Paraoanu described the quantum vacuum as an entity endowed with structure, which lies beneath the existential level of real matter[7] and cites Einstein's words - *"There is no such thing as an empty space, i.e. a space without field. Space-time does not claim existence on its own, but only as a structural quality of the field*". In previous papers we described the electron and pion tetrahedron models and various quark exchange reactions of the pion tetrahedrons including $\boldsymbol{\beta}$ decay and quark confinement[8-11].

In this paper we focus on a theory of the quantum vacuum structure filled with a pion tetrahedron tetraquark fabric. We note that the vacuum pion tetrahedrons are not ordinary matter since they are composed of 50% antimatter that "annihilates" the other 50% matter, however, the pion tetrahedrons have properties like mass, rotational and vibrational energy and electric dipole. Each lattice site contains a single tetraquark, $u\tilde{d}d\tilde{u}$, composed of two valence quarks and their antiquark pairs and having a tetrahedron structure. There are two pion tetrahedron chiral enantiomers obtained by exchanging the positions of two quarks at the tetrahedron vertices as shown below in line with Dirac/Weyl massless chiral spinors[1-5].

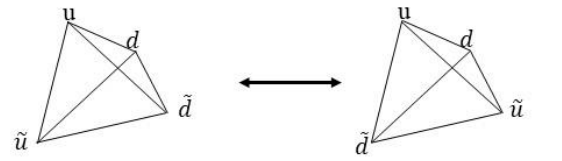

Left chirality *Right chirality*

Figure 1 illustrates the two pion tetrahedron enantiomers where the $\tilde{u}$ and $\tilde{d}$ antiquarks exchange positions.

We assume that the pion tetrahedron fabric in empty space may be a simple cubic lattice. However, in the vicinity of a massive star, the pion tetrahedron fabric may have a spherical symmetry with a cell size that changes according to the distance from the star. Each lattice site contains a single pion tetrahedron tetraquark, $u\tilde{d}d\tilde{u}$, composed of the two valence quarks and their antiquark pairs. The size of the tetrahedron edge may be a fraction of a femtometer while the pion tetrahedron lattice length in free space may be much larger, for example about $5.0 * 10^{-8}$ meter. In extreme gravitational fields, in the vicinity of a black hole for example, the pion tetrahedron lattice cell size may become extremely short, similar to the pion tetrahedron edge size of about $0.5 * 10^{-15}$ meter or less. Far away from any galaxy in the cosmic voids, the pion tetrahedron fabric may be extremely diluted. In the cosmic voids[12-14] the Modified Newton

Dynamics (MOND) low acceleration limit, $F = m\,\frac{a^2}{a_0}$, where a << a_0, may be obtained with $a \sim \frac{GM}{r}$ instead of Newton's acceleration $a = \frac{GM}{r^2}$ [9].

We assume that the pion tetrahedrons in each lattice site are massive and respond to gravitational field like a gas in gravitational field with exponential density drop[8]

$$\rho(r) = \rho(r_0)e^{\frac{-GM_S\, m_\pi\,(r-r_0)}{{r_0}^2 k_b\, T}} \qquad (1)$$

The pre-exponent density $\rho(r_0) = \frac{N}{V}$ may be estimated according to the mass of the black hole divided by the mass of a proton $N = \frac{M_{BH}}{M_p}$ divided further by the volume of the black hole Schwarzschild radius r_s cube or the star radius cube. We assume that the maximal density of the pion tetrahedron fabric is obtained when the number of pion tetrahedrons are equal to the number of protons in the star or the BH.

$$\rho(r_0) = \frac{N}{V} = \frac{3M_S}{M_p 4\,\pi\, r_S^3} \quad \frac{\#\,pions}{m^3} \qquad (2)$$

For the Milky way galaxy Sagittarius A black hole, the pion tetrahedrons density on its Schwarzschild radius is $6.55 * 10^{32}\ \frac{\#\,pions}{m^3}$ and for the sun on its surface it is $8.431 * 10^{29}\ \frac{\#\,pions}{m^3}$. For a single proton it is $7.799 * 10^{17}\ \frac{\#\,pions}{m^3}$, which is a huge number of pion tetrahedrons but still 6 orders of magnitude smaller than Avogadro's number $6.023 * 10^{23}$.

2. The Electron Model and the Quantum Vacuum

Electrons in the proposed quantum vacuum structure theory are non-elementary composed particles made of tetraquarks having two configurations we refer to herein as a right chiral $\tilde{u}\,du\tilde{u}$ and a left chiral $\tilde{u}\,dd\tilde{d}$. Adding an electron to the pion tetrahedron fabric is done by replacing one pion tetrahedron with one of the two chiral electron tetrahedrons and then using a double well potential Hamiltonian[15] that represents an exchange of quarks between the electron and the pion

tetrahedron on adjacent sites that transform the chiral electron tetrahedron to a pion tetrahedron and vice versa as shown in equation 1 below for a left chiral electron where the u *and* d quarks are exchanged as shown in figure 2 and equations 1 and 2 below.

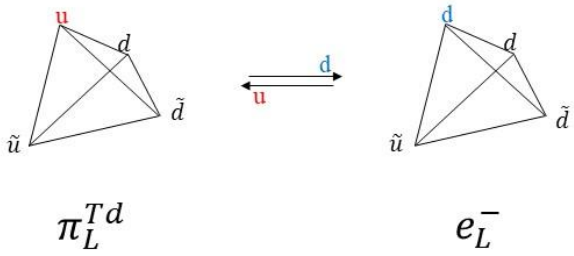

Figure 2 illustrates an electron and a pion tetrahedron where a single quark flavor is exchanged (u and d).

$$\tilde{u}d\tilde{d}u\,(\pi^{Td})_i + \tilde{u}d\tilde{d}d\,(e^L)_j \rightarrow \tilde{u}d\tilde{d}d\,(e^L)_i + \tilde{u}d\tilde{d}u\,(\pi^{Td})_j \qquad (1)$$

In the case of the right chiral electron the $\tilde{u}$ *and* $\tilde{d}$ antiquarks are exchanged, and the exchange reaction equation is

$$\tilde{u}d\tilde{d}u\,(\pi^{Td})_i + \tilde{u}d\tilde{u}u\,(e^R)_j \rightarrow \tilde{u}d\tilde{u}u\,(e^R)_i + \tilde{u}d\tilde{u}u\,(\pi^{Td})_j \qquad (2)$$

Since the quark exchange reactions are symmetric, the reactants on the left-hand-side and the products on the right-hand-side are identical, the usage of the double well potential Hamiltonian is justified[15].

$$\hat{H} = \frac{\hat{p}^2}{2m} + m\,\lambda\,(x^2 - a^2)^2 \qquad (3)$$

The mass m is the electron rest mass, a is the pion tetrahedron lattice cell size and the double well potential parameter λ determines the barrier height, $V_0 = m\,\lambda\,a^4$. Based on Dirac equation zitterbewegung force free trembling motion, we assume that in free space the potential barrier height $V_0 = \hbar\boldsymbol{\omega} = 2m_e c^2$, and hence the frequency $\omega = \frac{2m_e c^2}{\hbar}$ is equal to Dirac's equation zitterbewegung[16]. Accordingly, the approximate ground state energy inside the well $E_0 = \frac{1}{2}\hbar\boldsymbol{\omega} = m_e c^2 = 5.11 * 10^6\ eV$ is equal to the electron rest mass energy.

Figure 3 below illustrates the double well potential model for the electron and pion tetrahedron quark flavor exchange reaction in lattice sites i and j in the ground state. The quark exchange reaction and the double well potential is replicated between all adjacent lattice sites and the electron motion in the ground state is hence by quantum tunneling through the potential barrier V_0, which is twice the electron rest mass energy and represents the threshold for electron-positron pair production. Note that the electron tetraquark on both sides of the double well is identical and hence the electron configuration ($\tilde{u}\,dd\tilde{d}$ or $\tilde{u}\,du\tilde{u}$) is dynamically conserved while the quark exchanges occur with the zitterbewegung frequency.

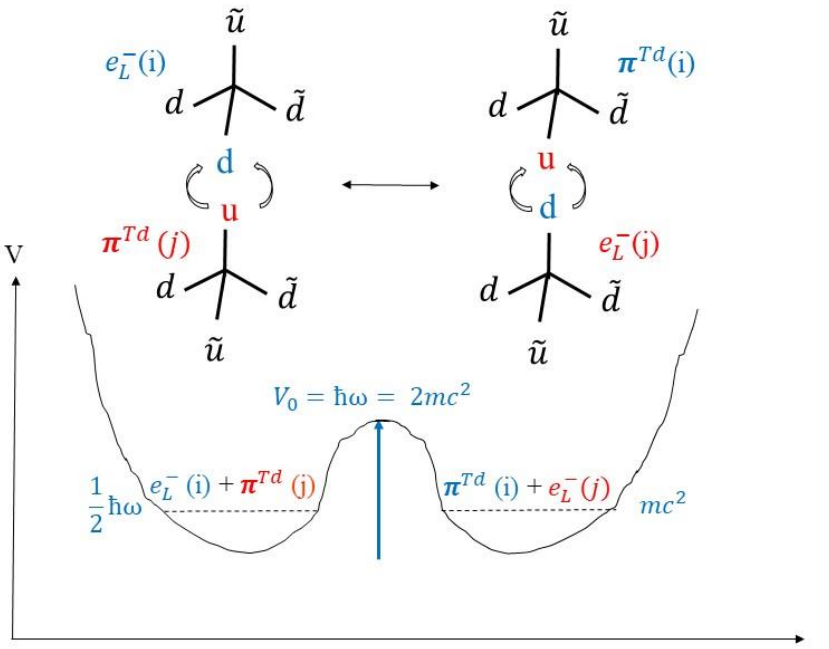

Figure 3 illustrates the double well potential model for the electron and pion tetrahedron quark flavor exchange reaction in lattice sites i and j in the ground state. Note that the potential barrier V_0 is twice the electron rest mass energy and represents the threshold for electron-positron pair production.

The tunneling probability, T, from the first to the second potential well in the ground state through the potential barrier is[15]

$$\mathrm{T} = e^{-\frac{8\,ma^3\sqrt{2\lambda}}{3\hbar}} = e^{-\frac{32V_0}{3\hbar\omega}} \qquad (4)$$

ω is the ground state frequency in each well separately given by

$$\omega = \frac{2\pi}{\tau} = \sqrt{8\,\lambda\,a^2} \qquad (5)$$

We may assume that the barrier height potential V_0 may vary in space according to the gravitational field for example and that $2m_ec^2$ is its absolute minimal value and accordingly we

may determine the electron velocity in space on the pion tetrahedron fabric. The velocity of the electron tetrahedron from site i to j due to the flavor exchange wave is calculated by the distance between the sites, a, divided by the time period, τ, and multiplied by the tunneling probability in the ground state T.

$$v_e = \frac{a}{\tau}\mathrm{T} = \frac{a\omega}{2\pi} e^{-\frac{32V_0}{3\hbar\omega}} \tag{6}$$

Since the electron velocity is limited by the speed of light, we get the following expression for the tunneling velocity from site to site.

$$\frac{a\omega}{2\pi} = c\, e^{\frac{32}{3}} \tag{7}$$

And an expression for the electron velocity.

$$\frac{v_e}{c} = e^{-\frac{32}{3}\left(\frac{V_0}{\hbar\omega} - 1\right)} \tag{8}$$

In the case that $V_0 = \hbar\boldsymbol{\omega}$ the electron velocity is maximal and equals to the speed of light, this means that in reality V_0 must be bigger than $\hbar\omega$.

The electron does not follow a classical trajectory, quarks are exchanged between the pion tetrahedron sites by tunneling through a potential barrier and effectively the motion of the electron creates a delocalized cloud. We assume that in some small Compton length range, $V_0 = \hbar\boldsymbol{\omega}$, and the electron speed may be equal to the speed of light as in Dirac's equation zitterbewegung and semi-classical electron models[16--17]. Out of this small region that may be in a shape of a ring or a torus, $V_0 > \hbar\boldsymbol{\omega}$, the electron speed is smaller than the speed of light. The double well potential barrier height for the quark flavor exchange in lattice sites i and j may be a function of the exchanged quark states $V_0\,(d_i, u_j)$. The pion tetrahedron quarks may rotate or vibrate with long range correlation creating local electric and magnetic fields since the quarks are electrically

charged. The double well potential with $\frac{V_0}{\hbar\omega} = 1.0$ and with $\frac{V_0}{\hbar\omega} = 2.0$ are shown below. With a larger potential barrier V_0 the wells are steeper, the tunneling probability through the barriers is smaller, the quark flavor exchange wave propagation is slower and the electron ground state wavefunction is more localized inside the well.

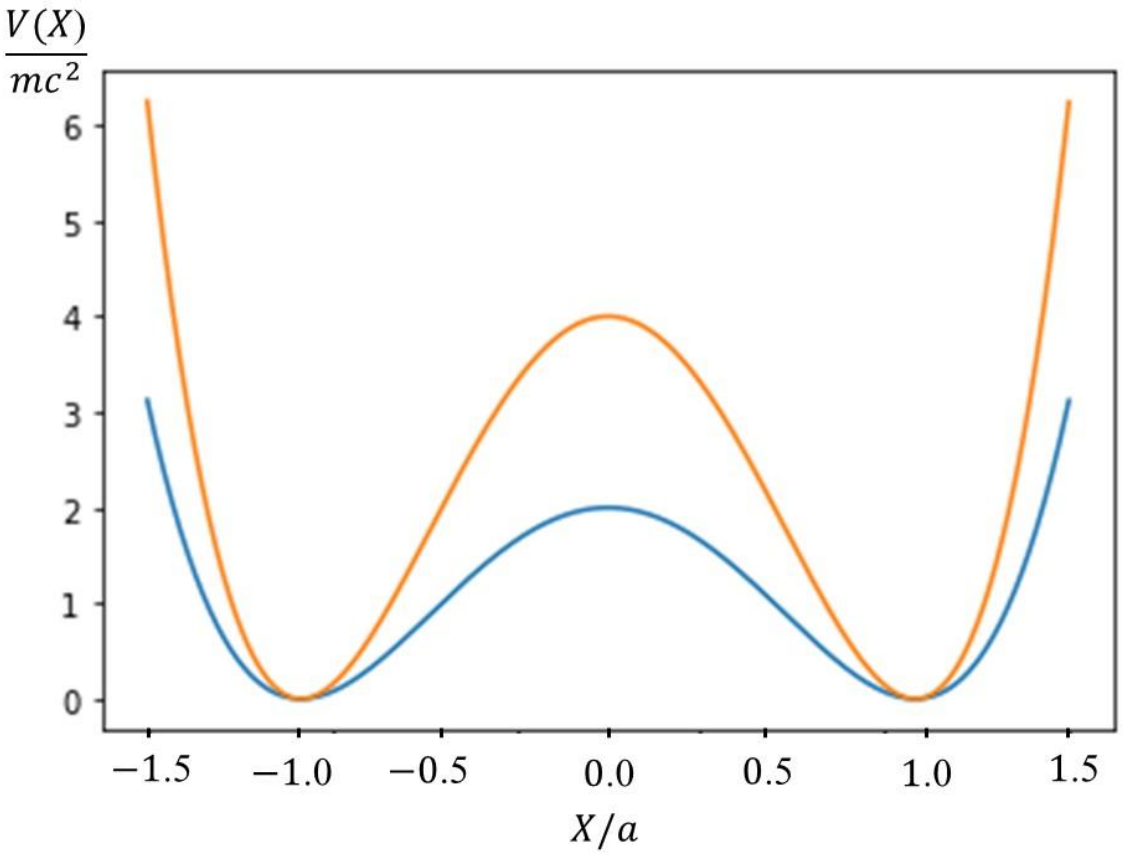

Figure 4 illustrates the double well potential with two values of the barrier height $V_0 = 2m_ec^2$ and $V_0 = 4m_ec^2$ with a = $5.2045 * 10^{-8}\ m$.

The frequency ω times the pion tetrahedron lattice cell length a is a constant (equation 7 above)

$$\omega\, a = 2\pi c e^{\left(\frac{32}{3}\right)} = 8.0811 * 10^{13} \qquad (9)$$

Using the zitterbewegung frequency, in the Compton region where the potential barrier height is minimal $V_0 = \hbar\boldsymbol{\omega}$, we can calculate the pion tetrahedron lattice cell length in free space

$$a = \frac{8.0811*10^{13}}{\omega} = \frac{\hbar\, 8.0811*10^{13}}{2m_e c^2} \text{ meter} \qquad (10)$$

$$a = \frac{8.0811*10^{13}}{1.5527*10^{21}} = 5.2045 * 10^{-8} \text{ meter} \qquad (11)$$

Note that with $V_0 = \hbar\boldsymbol{\omega}$, and the zitterbewegung frequency $\omega = \frac{2m_e c^2}{\hbar}$, the barrier height is $V_0 = 2m_e c^2$, which is the threshold for production of an electron-positron pair. The potential parameter λ is given by $\lambda = \frac{V_0}{m_e\, a^4} = \frac{2\, c^2}{a^4} = 2.4498 * 10^{46} \frac{1}{m^2 sec^2}$

The first order correction to the ground state energy of $E_0^{(0)} = \frac{1}{2}\hbar\boldsymbol{\omega}$ in the double well is[15]

$$E_0^{(1)} = \frac{3\hbar^2}{32 m_e a^2} = 2.637 * 10^{-6}\ eV \qquad (12)$$

The electron mass may be measured with high precision[18] where small deviations due to the time periodic variable interaction with the vacuum pion tetrahedron density may be measurable[11].

Assuming that the mass of the pion tetrahedron is about 6 orders of magnitude smaller than the electron, the pion tetrahedron density in free space may be estimated roughly.

$$\rho_{pion\ tetrahedron} = \frac{10^{-6}\, m_e}{(5.204*10^{-8})^3} = 6.46 * 10^{-15} \ \frac{k_g}{m^3} \qquad (13)$$

The estimated density of the Universe is $9.9 * 10^{-27} \frac{k_g}{m^3}$, which is equivalent to 5.9 protons in meter cube. Only 4.7% of the total density is due to visible matter which is about $4.33 * 10^{51} k_g$. The estimated volume of the visible Universe is $9.322 * 10^{78} m^3$. If we assume that the pion tetrahedron density in the Universe is uniform its mass will be about $6.023 * 10^{64}\ k_g$, 13 orders

of magnitude larger than the visible mass. However, we assume that the pion tetrahedron density is denser close to matter particles and is extremely diluted far from matter for example in the cosmic web voids. The pion tetrahedron mass in the Universe is probably much smaller than $6.023 * 10^{64}\ k_g$, still, due to the huge volume of the Universe, the pion tetrahedron mass should not be neglected.

3. The β Decay and the Electron Model

We assumed that electrons are composed of tetraquarks, and we did not attempt to provide a proof for the electron model[8-11]. Here we want to show that the β rays, which were discovered in 1899 by Ernest Rutherford, give a significant support for the proposed quark content of the electron tetrahedron model. In 1900, Becquerel measured the mass-to-charge ratio (m/e) for radioactive β particle emission and found that m/e ratio for β particles is the same as Thomson's cathode ray electrons and suggested that β rays are electrons[19-20]. At that time, protons and neutrons and their internal structure were not known and the question how an electron is emitted from a nucleus made of protons and neutrons that contains quarks and gluons only[6] could not be asked. We propose to write down a quark based β decay equation assuming that the valence quarks and antiquarks are conserved.

$$udd\ (n) + u\tilde{d}d\tilde{u}\ (\pi^{Td}) \rightarrow udu\ (p^{+}) + \tilde{u}\ d\ \tilde{d}d\ (e_L^{-}) + \tilde{\nu}_\sigma \qquad (14)$$

Note that the β decay according to equation 14 describes a second order kinetic reaction where a collision between a neutron and a pion tetrahedron triggers the quark exchange reaction. The second order kinetics classification is important since if the density of the pion tetrahedrons is reduced, for example in the cosmic voids, the rate of the β decay will be reduced too. Hence the β decay rection rate is not a first order kinetic constant and it should depend on the pion tetrahedrons density that drops like the atmospheric density drops away from earth surface[8].

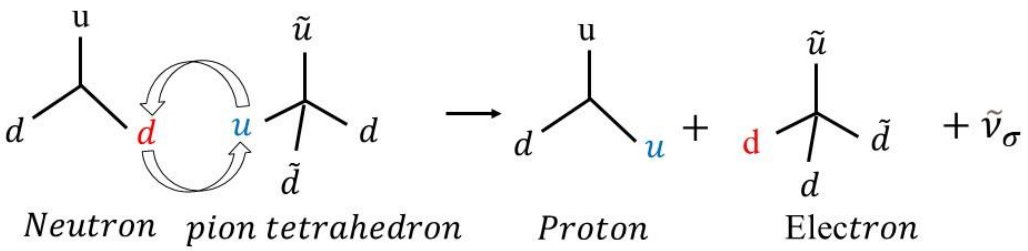

Figure 5 illustrates the $\boldsymbol{\beta}$ decay as a quark exchange reaction between a neutron and a pion tetrahedron as a second order kinetics reaction.

The electron tetrahedron $\tilde{u}\,d\tilde{d}d\,(\,e_L^-)$ and the anti-neutrino $\tilde{\nu}_\sigma$ are energetic spin half fermions that propagate on the pion tetrahedron fabric. The electron tetrahedron propagates via quark exchange reactions that occur by tunneling through the double well potential barrier while the anti-neutrino propagation may be an internal motion of the pion tetrahedrons degrees of freedom in each lattice site, a vibration or rotation waves that propagate in almost the speed of light on the pion tetrahedron fabric.

Note that the second configuration right chiral electron, $d\tilde{u}\,u\tilde{u}$, described above in equation 2, is not obtained by the $\boldsymbol{\beta}$ decay according to equation 14, which means that the $\boldsymbol{\beta}$ ray electrons are created with specific chirality as observed experimentally by C. S. Wu in 1957[19-20]. The proposed electron tetrahedron model made of tetraquarks and the $\boldsymbol{\beta}$ decay quark equation 14

with the assumed quark conservation rule provides a reaction mechanism for the $\boldsymbol{\beta}$ decay process that includes the chirality of the emitted electrons and also predicts a second order kinetics and a dependence on the gravitational field of the decay rate that may be observed[8].

The β^+ decay transform a proton to a neutron and emits a positron with the opposite chirality comparing to the electron emitted in the β^- decay. The β^+ decay is a third order kinetic reaction triggered by a neutrino and a pion tetrahedron and it also conserve the valence quark numbers that are only rearranged differently in both reactions.

$$udu\ (p^+) + u\tilde{d}d\tilde{u}\ (\pi^{Td}) + \nu_\sigma \rightarrow udd\ (n) + u\tilde{d}u\tilde{u}\ (e_R^+) \qquad (15)$$

4. The Positron Model and the Quantum Vacuum

We assume that positrons are tetraquark tetrahedrons like the electron tetrahedrons but having a $u\ \tilde{d}$ quark pair with a plus charge instead of the $\tilde{u}\ d$ quark pair with a negative charge for the electron as shown below in figures 6 (a-b) for the electrons on the left and figures 6 (c-d) for the positrons on the right. Two positron configurations can be described with right and left chirality like the electrons and have additional $d\ \tilde{d}$ or $\tilde{u}\ u$ quark pairs as shown below in figures 6 (c-d) on the right.

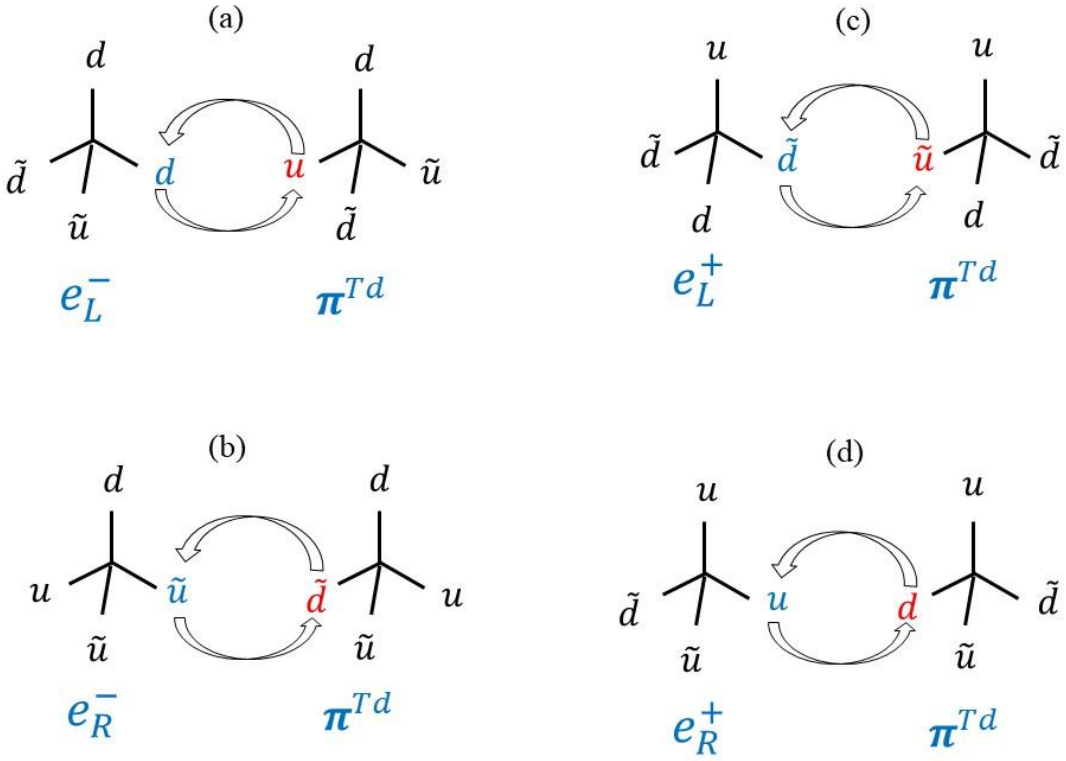

Figure 6 illustrates electron tetrahedrons (a) and (b) and positron tetrahedrons (c) and (d) exchanging quarks with pion tetrahedrons with symmetric reactions such that the electrons and positrons transform to pion tetrahedrons and vice versa in each exchange reaction.

5. Electron-Positron Condensation

Electron-positron annihilation according to the theory of the quantum vacuum structure is a condensation of an electron tetrahedron and a positron tetrahedron into two pion tetrahedrons that become part of the quantum vacuum structure fabric as shown in equation 16 below.

$$\tilde{u}d\tilde{d}d(\,e_L^-) + u\tilde{d}\tilde{u}u(\,e_R^+) \;\rightarrow\; \tilde{u}du\tilde{d}(\pi^{Td}) + \tilde{d}d\tilde{u}u\,(\pi^{Td}) \qquad (16)$$

Hence if an electron tetrahedron in site i on the lattice collide with a positron on site j on the lattice the outcome is that in both sites i and j after the collision will become two pion

tetrahedrons. The electron and positron are annihilated and energy is transferred to the pion tetrahedron fabric as excitations that propagate on the fabric as two electromagnetic waves.

6. Electron Pairs and Pauli Exclusion Principle

An electron-electron pair may be created by forming a pion tetrahedron that acts a QCD glue as shown in equation 17 below. The chirality/spin of the pair is opposite creating a Cooper pair according to Bardeen-Cooper-Schrieffer (BCS) superconductivity theory[21].

$$\tilde{u}d\tilde{d}d(\,e_L^-) + \,\tilde{u}d\tilde{u}u(\,e_R^-) \;\rightarrow\; \tilde{u}d\tilde{d}d\tilde{u}u\,\tilde{u}d\big(e - e_{\downarrow\uparrow}^{pair}\,\big) \qquad (17)$$

According to BCS theory the electron pairing interaction is mediated by phonons, the motion of the solid-state lattice ions, that creates the attraction between the electron pairs. Here we suggest that the pion tetrahedron acts like a QCD glue connecting the electron pairs in addition to the contribution of the observed lattice phonons, e.g. the isotopic effect. Hence, without phonons the pion tetrahedron interaction is too small and is not strong enough to bind the electron pair in a solid.

We propose further that the electron-electron pair interaction described in equation 17 via the pion tetrahedron QCD glue may be the underlying electron pair attraction mechanism in chemical bonds in atoms and molecules where the pion tetrahedron fabric is denser. When two electron tetrahedrons with opposite chirality collide in site i and j in the dense pion tetrahedron fabric, they are attracted to each other by the formation of the pion tetrahedron QCD glue and they will continue a correlated pair motion on the dense pion tetrahedron fabric. The interaction is a pair attraction, a third electron cannot correlate similarly with the electron pair and this mechanism may be the underlying mechanism for the Pauli exclusion principle[22].

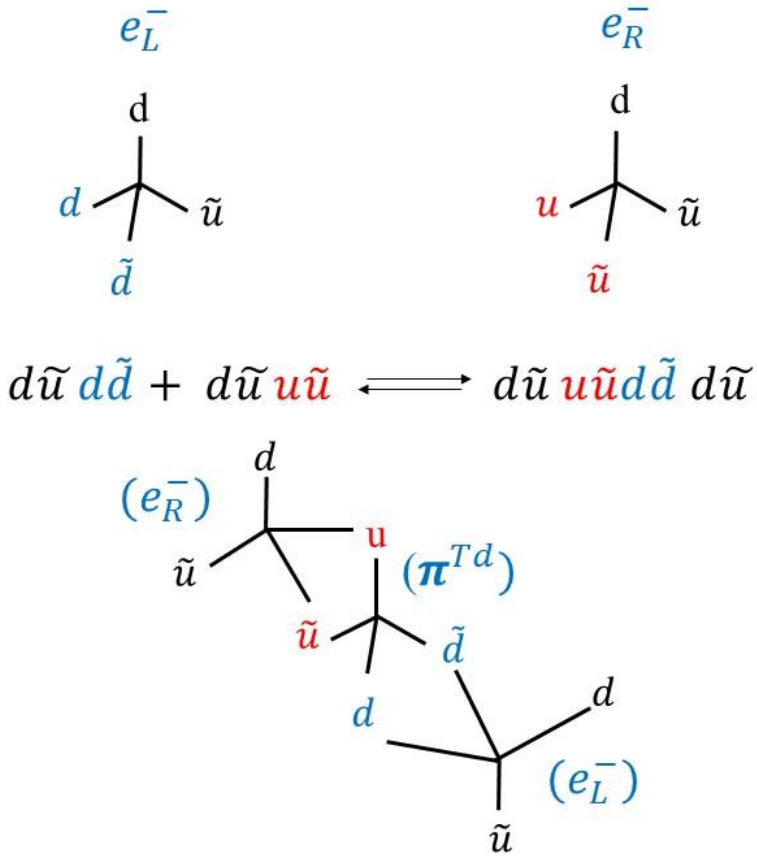

Figure 7 illustrates electron pairing mechanism forming a pion tetrahedron that acts like a QCD glue

7. The Proton Model and the Quantum Vacuum Valence Quarks

A proton on site i and a pion tetrahedron on site j may exchange three quarks according to equation 18(a-b) below where the proton with left or right chirality is transformed to a pion tetrahedron and vice versa. The quark structure and chirality are conserved in both reactions.

$$ud\,uu\tilde{u}\ (p_R^+) + u\tilde{d}\,d\tilde{u}\,(\pi^{Td}) \rightarrow ud\tilde{d}\,\tilde{u}\,(\pi^{Td}) + ud\,uu\tilde{u}\,(p_R^+) \qquad (18a)$$

$$ud\,ud\tilde{d}\ (p_L^+) + ud\tilde{d}\,\tilde{u}\,(\pi^{Td}) \rightarrow ud\tilde{u}\,\tilde{d}\,(\pi^{Td}) + ud\,ud\tilde{d}\,(p_L^+) \qquad (18b)$$

Note that the reactions are symmetric and may be modeled with a double well potential similar to the electron and pion tetrahedron above, however, the potential barrier is higher now, $2m_pc^2$.

Similar quark exchange reaction can be written for a neutron and the motion of the matter particles, electrons, positrons, protons and neutrons on the proposed vacuum pion tetrahedron fabric is performed by quark exchange reactions between lattice sites that occur with quantum tunneling through a potential barrier. Note that the decomposition of the spin of the proton has been the subject of tremendous interest since the discovery that the intrinsic spin carried by quarks was only about $\lesssim 10\% - 30\%$ of the proton's spin[23]. We propose here that the proton structure includes a $d\tilde{d}$ or a $u\tilde{u}$ mesons as shown below that determines the proton chirality and contribute energy and spin to the proton.

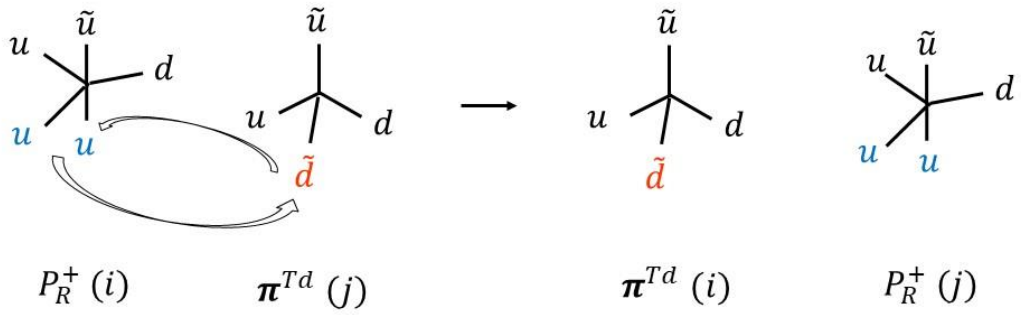

Figure 8 illustrates a proton and a pion tetrahedron quark exchange reaction transforming the proton to a pion tetrahedron and vice versa on the vacuum lattice sites i and j. Note that the right chiral proton structure includes a $u\tilde{u}$ meson.

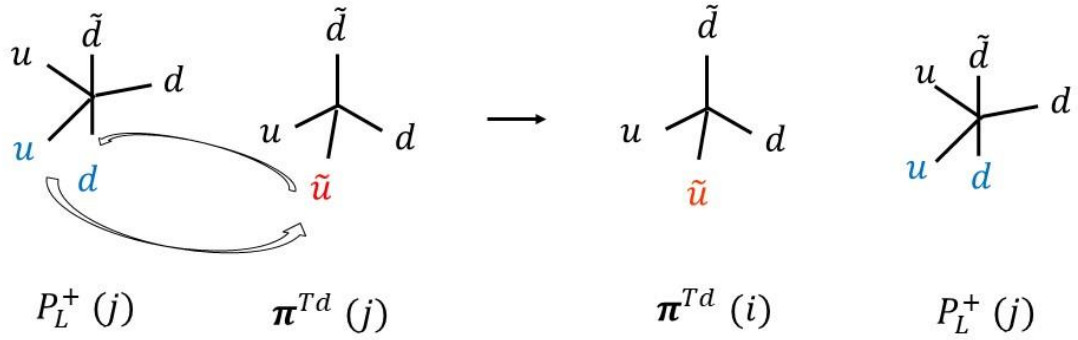

Figure 9 illustrates a proton and a pion tetrahedron quark exchange reaction transforming the proton to a pion tetrahedron and vice versa on the vacuum lattice sites i and j. Note that the left chiral proton structure includes a $d\tilde{d}$ meson.

8. The Pion Tetrahedron Nuclear Glue

The pion tetrahedrons may act as a QCD nuclear glue between a proton and neutron in a deuterium nucleus for example as illustrated in figure 10 and 11 below. The pion tetrahedron allows a double quark exchange between the two hadrons that transform the proton to a neutron and vice versa.

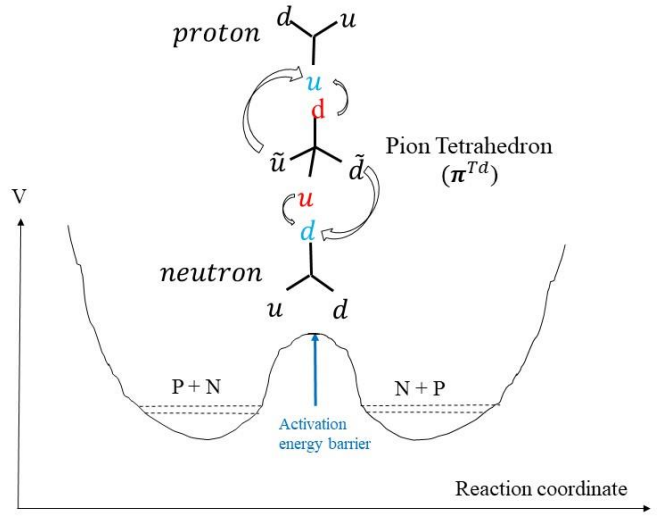

Figure 10 illustrates a proton and a neutron exchanging quarks with a pion tetrahedrons that acts like a QCD glue. Since the quark exchange reaction is symmetric transforming the proton to a neutron and vice versa, a double well potential is created.

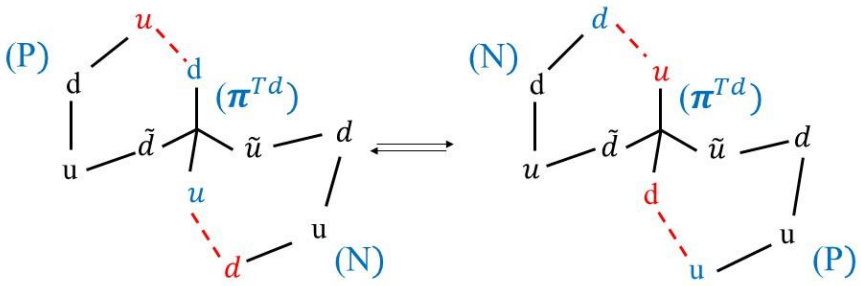

Figure 11 illustrates a proton and a neutron exchanging quarks with a pion tetrahedrons that acts like a QCD glue that provides the quarks for the double exchange reaction.

9. BH Superradiance

Active Galactic Nuclei's (AGNs) are the most powerful energy sources in the Universe, however, the engine powering the AGN jets is still largely unknown. Superradiance occurs due to spontaneous particle-antiparticle pair creation[24]. The particle-antiparticle pairs are created in the vicinity of a potential barrier, and in the case of a BH, in the vicinity of the event horizon. With Superradiance, at low energy comparing to the potential barrier, all particles incident on the potential barrier are reflected, however the incident beam stimulates pair creation at the barrier and particles join the enhanced reflected beam, while the negative transmitted current can be interpreted as a flow of antiparticles with charge -e. All the particles incident with energy ω are reflected with energy ω and in addition, because of pair creation, more particles with charge e and energy ω join the enhance Superradiance reflected beam. For each additional particle another one with charge -e is transmitted through the event horizon to the BH and transmits its energy -ω to the BH. The Superradiance creates a reflection gain. The BH event horizon behaves as a viscous one-way membrane where the BH ergoregion allows extracting energy from the vacuum.

Brandt describes the topic of quasi-periodic eruptions and oscillations at the end of lecture 3[25]. The quasi-periodic x-ray eruption (QPE) sources show recurrent phases of activity with recurrence times as short as a few hours to a day and may be as long as hundreds to a thousand days[26]. Quasi-periodic oscillations (QPOs) in the x-ray emission of blazars may be due to disk-jet interactions, either due to an accretion disc limit cycle, jet instabilities or helical motions[27]. QPEs were detected from the nucleus of galaxy GSN 069 and active galaxy RX J1301.9+2747. Rapid and recurrent increases of the X-ray count-rate by more than one order of magnitude were detected[28]. The QPE underlying physical mechanism is a topic of heated debate where most models propose that the QPEs originate either from instabilities within the inner accretion flow

or from orbiting objects[29]. Janiuk et al studied strong quasi-periodic flare-like events on timescales of tens of seconds[30]. Ingram and Mota review the quasi-periodic oscillations from black hole X-ray binaries observation and theory, where the QPOs statistical properties are described with special attention to the Lense-Thirring relativistic precession model[31].

Below we describe an AGN Carnot engine that extracts energy from the ergoregion pion tetrahedron fabric of the vacuum and generates a mass and energy gain that may expand the quantum vacuum pion tetrahedron fabric of the Universe from inside like a balloon.

10. AGN Carnot Engine and Pion Tetrahedron Fabric

Abramowicz and Struab describe analytic models for Kerr BH thin accretion disc[36-39]. Shakura and Sunyaev using the thin disc expansion parameter $\frac{H}{R} \ll 1$, derived the Newtonian hydrodynamical model of stationary and axially symmetric thin accretion discs by introducing 12 equations[36]. Accordingly, the accretion disc density ρ is a function of the radius r and three main parameters, $\rho(r, M, \dot{M}, \alpha)$, where M is the BH mass, $\dot{M}$ is the accretion rate and α is a viscosity parameter.

For a thin accretion disc, the density ρ is assumed to vanish at the inner edge of the accretion disc at r_0[36].

$$\rho(r, M, \dot{M}, \alpha) = 3.1 * 10^{-8}\, \alpha^{-7/10}\, \dot{M}_{16}^{11/20} M_{BH}^{5/8}\, R_{10}^{-15/8}\, f(r)^{11/5} \quad \frac{gr}{cm^3} \tag{20}$$

$$\mathrm{H}(r, M, \dot{M}, \alpha) = 1.7 * 10^{3}\, \alpha^{-1/10}\, \dot{M}_{16}^{3/20} M_{BH}^{-3/8}\, R_{10}^{9/8}\, f(r)^{3/5} \quad cm \tag{21}$$

$$\mathrm{f}(r) = \left(1 - \sqrt{\frac{r_0}{r}}\right)^{1/4} \tag{22}$$

$\dot{M}_{16}$ is the accretion rate, in units of $10^{16}\ \frac{gr}{sec}$, M_{BH} is the mass of the central accreting object, in units of a solar mass, R_{10} is the radial location in the disc, in units of 10^{10} cm. The AGN Carnot

engine model described herein uses the thin accretion disc density and pressure analytic expressions of equations 20-22 for calculating the work done by the AGN Carnot engine.

Corley and Jacobson[33] showed that in the presence of an inner and an outer horizon the negative energy partners of Hawking quanta return to the outer horizon and stimulate more Hawking radiation if the field is bosonic. This process leads to exponential growth of the bosonic radiated flux and correlations among the quanta emitted at different times, unlike in the usual Hawking effect. Next the exponentially duplicated pion tetrahedron bosons may split according to equations 23a-d below releasing a lot of heat and additional particles may be emitted to space with extremely high energy by the huge relativistic jets in pulses[34]. Similarly, BH Superradiance can create a reflection gain where the BH ergoregion allows extracting energy from the vacuum[24].

We previously assumed that matter and antimatter may be separated on the event horizon of black holes (BH) by the Hawking radiation process[32]. Due to the high density of the pion tetrahedron fabric close to the BH event horizon, the distance between the pion tetrahedrons may become less than a femtometer and then a transition state complex of two or even four pion tetrahedrons may be created and next may be separated into matter and antimatter hadrons. The matter hadrons are emitted to space with huge energy and the antimatter remains trapped under the horizon of the black hole according to Hawking radiation process. Equation 23a-d show how neutrons, protons, deuteriums and electrons may be generated by two and four pion tetrahedrons.

$$2\,u\tilde{d}d\tilde{u} \rightarrow\ udd\tilde{u}u(n)\ +\ \tilde{d}\tilde{u}\,\tilde{d}(\tilde{n}) \qquad (23a)$$

$$2\,u\tilde{d}d\tilde{u} \rightarrow\ udu\tilde{d}d(p)\ +\ \tilde{d}\tilde{u}\,\tilde{u}(\tilde{p}) \qquad (23b)$$

$$4\,u\tilde{d}d\tilde{u}\,d \rightarrow\ udd\tilde{d}d\ uudu\tilde{u}\,(deuterium) +\ \tilde{d}\tilde{u}\,\tilde{d}\tilde{u}\tilde{d}\tilde{u}\,(\,antideutrium) \qquad (23c)$$

Next, neutrons may collide with pion tetrahedrons and split into protons, electrons and anti-neutrinos via the second order kinetics $\boldsymbol{\beta}$ decay[8] -

$$udd\tilde{u}u\ (n) + u\tilde{d}d\tilde{u}\ (\pi^{Td}) \rightarrow uduu\tilde{u}\ (\ p^{+}) + \tilde{u}\ d\ \tilde{d}d\ (\ e_{L}^{-}) +\ \tilde{\nu}_{\sigma} \qquad (23d)$$

The AGN system may act as a Carnot engine working between cold and hot reservoirs[35] as described in figure 12 below. The cold reservoir is the BH with Hawking temperature, $T_C = \frac{\hbar c^3}{8\pi G M_{BH} K_b}$, and the hot reservoir is the AGN accretion disc temperature $T_h = \left(\frac{3G\ M_{BH}\ \dot{M}}{\pi\ \sigma_{SB} r^3}\right)^{1/4}$, for the AGN systems T_h is 5 order of magnitude and more bigger than T_c.

We assume that the pion tetrahedron fabric in the BH ergoregion play the role of the Carnot engine gas that expands and is compressed and extract work from the temperature difference between the hot accretion disc and the BH cold reservoirs. The BH accretion disc play the role of the Carnot engine piston that compress the pion tetrahedron gas in the ergosphere. The AGN Carnot engine produces an overall mass gain, creating and emitting mass and energy to space. Note that the pion tetrahedrons are bosons and that the anti-particle of the pion tetrahedron is a pion tetrahedron and hence a pair of pion tetrahedrons may be created in the BH ergoregion, one will be reflected to space and the other will fall in below the BH event horizon according to the Hawking process. Note that the proposed model generates the pion tetrahedrons from the ergosphere quantum vacuum using the temperature difference between the two reservoirs and it does not reduce the mass of the BH or the mass accreted from the disc.

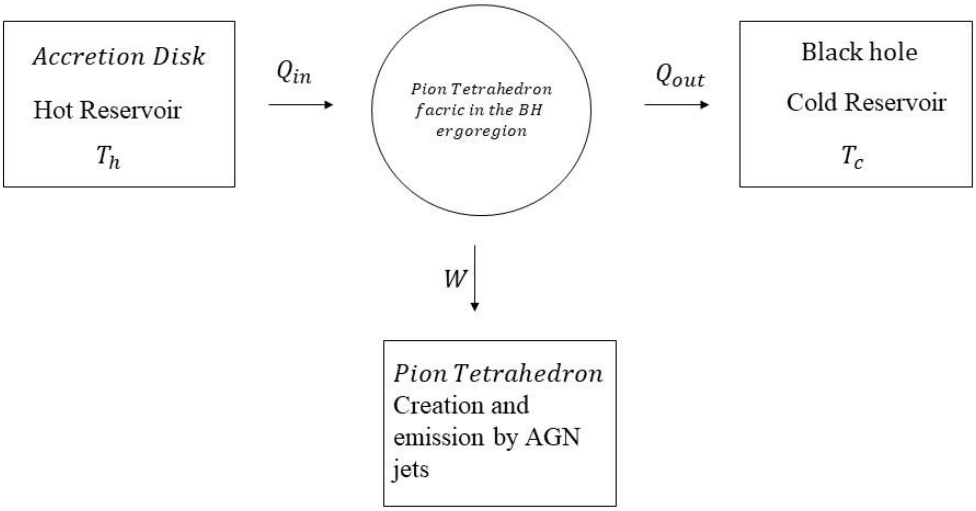

Figure 12 illustrates the AGN Carnot engine. The AGN Carnot engine working gas is the quantum vacuum pion tetrahedrons fabric in the BH ergoregion. The ergoregion acts like an engine piston housing where the accretion disc acts as the piston. Pion tetrahedrons produced by the Carnot engine are emitted to space in pulses by the AGN jets.

The Carnot cycle is described below with a four-step pressure-volume (P-V) diagram shown in figure 13. The work that may be transformed to mass emitted to space by the AGN jets and the energy that may heat up the corona at the jet base is given by the integral $W = \oint PdV$.

The Carnot cycle first step is **isothermal expansion** that starts from the pion tetrahedron pairs split on the static event horizon and elevates pion tetrahedrons from the event horizon r_s to a second elevated position we determine using Shakura and Sunyaev model. Using the thin accretion disc analytic expressions for the mass density and height[36,37] we can calculate the work done by the pion tetrahedron gas pushing back the accretion disc material. The work integral in the gravitational field of the BH is given on the right-hand-side of equation 24.

$$W_{A-B} = n_\pi RT_h \ln\frac{V_B}{V_A} = 2\pi \int_{r_a}^{r_b} \frac{GM_{BH}H(r)\rho(r)r}{r^2} dr \quad (24)$$

Using equation 24 we can calculate the number of pion tetrahedron moles of gas n_π are needed to push back the thin accretion disc matter.

$$n_\pi = \frac{2\pi \int_{r_a}^{r_b} \frac{GM_{BH}H(r)\rho(r)r}{r^2} dr}{RT_h \ln\frac{V_B}{V_A}} \quad (25)$$

The second expansion step is **adiabatic expansion** from V_B to V_C

$$W_{B-C} = n_\pi C_V (T_c - T_h) \quad (26)$$

The third step is **isothermal compression from** V_C to V_D by the external pressure of the accretion disc.

$$W_{C-D} = n_\pi RT_c \ln\frac{V_C}{V_D} = 2\pi \int_{r_d}^{r_c} \frac{GM_{BH}H(r)\rho(r)r}{r^2} dr \quad (27)$$

The last step is **adiabatic compression** from V_D to V_A where the pion tetrahedron pairs are created by the BH laser effect or the BH Superradiance process and the step work is given by

$$W_{B-C} = n_\pi C_V (T_h - T_c) \quad (28)$$

The total work done by the AGN Carnot engine is determined mainly by the first term due to the huge difference between the accretion disc temperature T_h and the BH T_c.

$$W_{AGN} = n_\pi RT_h \ln\frac{V_B}{V_A} - n_\pi RT_c \ln\frac{V_D}{V_C} \quad (29)$$

If we assume that most of the AGN Carnot engine energy is transformed into pion tetrahedron production by the Superradiance process or the BH laser effect, the mass of the pion tetrahedrons m_π may be calculated from equations 25 and 29

$$n_\pi m_\pi c^2 = W_{AGN} \quad (30)$$

$$m_\pi = \frac{W_{AGN}}{n_\pi c^2} \quad (31)$$

For AGN system with a billion sun masses and an accretion rate of $10^{25}\ \frac{gr}{cm^3}$ the pion tetrahedron mass according to equations 25 and 31 is $3.767 * 10^{-35}$ kg, about $4.135 * 10^{-5}$ smaller than the electron mass. The integral in equation 25 is calculated with $r_a = \frac{2.0\ GM}{c^2}$ and $r_b = \frac{2.63\ GM}{c^2}$, where r_b is the radius of the maximal accretion disc density ρ_{max}[36]. The calculated number of pion tetrahedrons that may be produced by the supermassive AGN system in the Carnot cycle is huge, $8.0137 * 10^{43}$, 20 order of magnitude bigger than the Avogadro number, $6.022 * 10^{23}$. This impressive number means that over time and by many such supermassive AGN system Carnot engines, the universe may be filled gradually by more and more pion tetrahedrons that form the expanding quantum vacuum fabric of the universe.

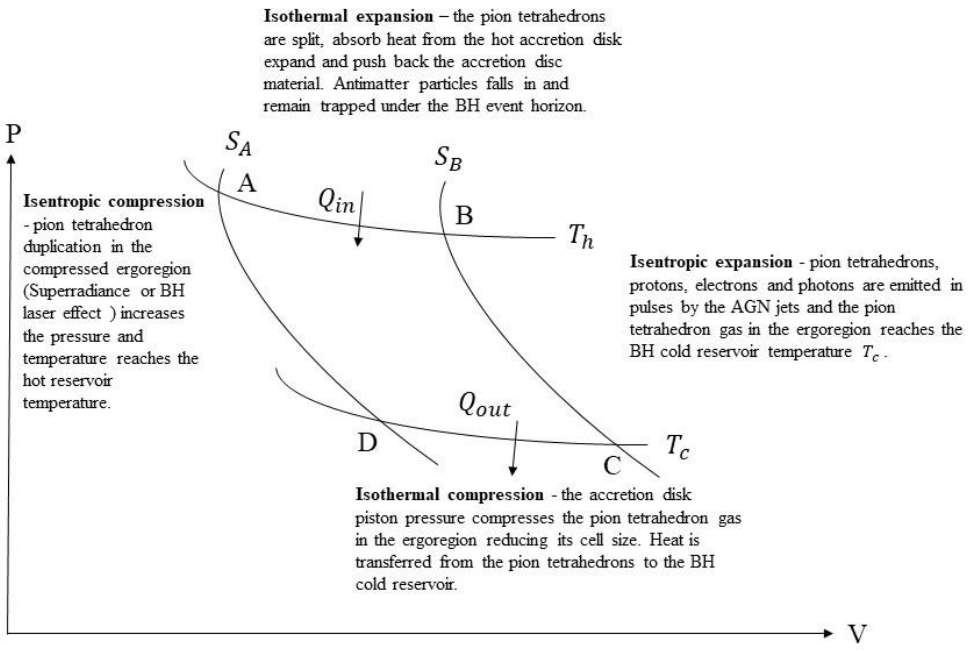

Figure 13 illustrates the four step AGN Carnot engine in a P-V diagram. Creation of pion tetrahedrons occurs in step DA and emission to space in step BC.

Note that the Carnot cycle does not define a specific time period and assumes that the cycle time is slow enough such that thermal equilibrium is maintained. However, for the AGN Carnot engine having the rotating accretion disc we have a natural definition for the cycle time, $T_P = \frac{2\pi}{\Omega_k}$ where $\Omega_k = \frac{1}{r_s}(\frac{GM}{r_s})^{\frac{1}{2}}$ is the Keplerian rotation frequency at the inner edge. For a 1 million sun masses BH, Ω_k is 0.1 sec^{-1} and hence the Carnot engine period would be 61.9 seconds.

Does the Universe expand by stretching or by creating space? [39] Siegel's answer is that both occurs, matter is diluted by the stretching of space and new spaces are created by the vacuum dark energy. The proposed pion tetrahedron fabric and the AGN Carnot engine may do both by the duplication of pion tetrahedron bosons in the BH ergoregions and their emission to space that expands the pion tetrahedron fabric of the quantum vacuum from inside like a balloon.

11. Summary

According to the proposed theory of the quantum vacuum fabric structure, pion tetrahedron fabric fills space with varying density that depends on the matter included in each space region. The pion tetrahedron fabric allows propagation of massive particles, electrons, positrons, protons and neutrons via rapid quark exchange reactions with the zitterbewegung frequency, and massless particles via vibrations and rotations of the pion tetrahedron fabric with no quark exchanges. The theory of the quantum vacuum fabric structure assumes that the valence quarks and antiquarks, $u, d, \tilde{u}, \tilde{d}$ are the building blocks of the Universe and that other stable and unstable particles are comprised from various combinations of the valence quarks. The proposed AGN Carnot engine creates and emits pion tetrahedrons to space by the AGN jets in pulses. A mechanism for the expansion of the Universe may be the duplication and emission to space of the quantum vacuum pion tetrahedrons by the AGN Carnot engines that expands the Universe

quantum vacuum pion tetrahedron fabric from inside like a balloon. Shakura and Sunyaev thin accretion disc analytic expressions[36] are used for calculating the pion tetrahedron mass and the number of pion tetrahedrons emitted by the AGN Carnot engine in a cycle.

References

[1] Lee, T., (2012), "Vacuum quark condensate, chiral Lagrangian, and Bose-Einstein statistics", https://arxiv.org/abs/1206.1637

[2] Brodsky, S. B., Shrock, R., (2008), "On Condensates in Strongly Coupled Gauge Theories", https://arxiv.org/abs/0803.2541

[3] Brodsky, S. B., Roberts, C. D., Shrock, R., Tandy, P.C., (2010), "Essence of the vacuum quark condensate", https://arxiv.org/abs/1005.4610

[4] Buballa, M., Carignano, S., (2014), "Inhomogeneous chiral condensates", https://arxiv.org/abs/1406.1367

[5] Byers, N., (1998), "E. Noether's Discovery of the Deep Connection Between Symmetries and Conservation Laws", https://arxiv.org/abs/physics/9807044

[6] Burkert, V.D. et al, (2022), "Precision Studies of QCD in the Low Energy Domain of the EIC", https://www.researchgate.net/publication/365850432_Precision_Studies_of_QCD_in_the_Low_Energy_Domain_of_the_EIC

[7] Paraoanu, G.S., (2014), "The Quantum Vacuum", https://arxiv.org/abs/1402.1087

[8] Rom, R., (Apr 2023), "The Quantum Chromodynamics Gas Density Drop and the General Theory of Relativity Ether", Journal of High Energy Physics, Gravitation and Cosmology, 9, No. 2. https://www.scirp.org/journal/paperinformation.aspx?paperid=124153

[9] Rom, R., (Apr, 2024), "Non-Uniform Pion Tetrahedron Aether and Electron Tetrahedron Model", Journal of High Energy Physics, Gravitation and Cosmology. https://www.scirp.org/journal/paperinformation?paperid=132602

[10] Rom, R., (Jan 2024), "The Pionic Deuterium and the Pion Tetrahedron Vacuum Polarization", Journal of High Energy Physics, Gravitation and Cosmology, 10, No. 1. https://www.scirp.org/journal/paperinformation?paperid=130928

[11] Rom, R., (May 2024), "QCD's Low Energy Footprint", https://vixra.org/abs/2403.0128

[12] Keenan, R.C., Barger, A.J, Cowie, L.L., (2013) "EVIDENCE FOR A ~300 MEGAPARSEC SCALE UNDER-DENSITY IN THE LOCAL GALAXY DISTRIBUTION", The Astrophysical Journal, 775:62 (16pp), 2013, September 20.

[13] Banik, I., (Nov 20, 2023), "Do we live in a giant void? It could solve the puzzle of the Universe's expansion", https://theconversation.com/do-we-live-in-a-giant-void-it-could-solve-the-puzzle-of-the-universes-expansion-216687#:~:text=When%20we%20measure%20the%20expansion,area%20with%20below%20average%20density).

[14] Mazurenko, S., Banik, I., Kroupa, P., Haslbauer, M., (Nov 20, 2023), "A simultaneous solution to the Hubble tension and observed bulk flow within 250 h −1 Mpc", https://arxiv.org/abs/2311.17988

[15] Grabovsky, D, (2021), "The Double Well", https://web.physics.ucsb.edu/~davidgrabovsky/files-teaching/Double%20Well%20Solutions.pdf

[16] Santos, I. U., (2023), "The zitterbewegung electron puzzle", https://www.researchgate.net/publication/374257062_The_zitterbewegung_electron_puzzle

[17] Davis, B.S., (2020), "Zitterbewegung and the Charge of an Electron", https://arxiv.org/abs/2006.16003

[18] Sturm, S., et al, (2014), "*High-precision measurement of the atomic mass of the electron"*, https://arxiv.org/abs/1406.5590

[19] Frauenfelder, H., et al,(Apr, 1957), "Parity and the Polarization of Electrons from Co60", Phys. Rev. 106, 386.

[20] Lashomb, P.R, (Thesis, 2015), "MEASURING PARITY VIOLATION IN COBALT-60 DECAY", https://dspace.houghton.edu/server/api/core/bitstreams/2c5d4610-06ad-43c1-b4fe-beb8e92c9e39/content

[21] Bardeen, J., Cooper, L.N., Schrieffer, J.R., (1957), "Theory of Superconductivity", Phys. Rev. 108, 1175. https://journals.aps.org/pr/abstract/10.1103/PhysRev.108.1175

[22] Kaplan, I. G., (2019). "Pauli Exclusion Principle and its theoretical foundation", https://arxiv.org/pdf/1902.00499

[23] Karpie, J., et al, (2024), "Gluon helicity from global analysis of experimental data and lattice QCD Ioffe time distributions", https://arxiv.org/abs/2310.18179

[24] Brito, R., Cardoso, V., Pani, P., (2021), "Superradiance", https://arxiv.org/pdf/1501.06570

[25] Brandt, N., (2024), "An Observational Overview of Active Galactic Nuclei", https://www.youtube.com/watch?v=zFv03n_hdfc

[26] Guolo, M. et. al., (2024), “X-ray eruptions every 22 days from the nucleus of a nearby galaxy”, https://arxiv.org/abs/2309.03011

[27] Smith, E., Orama, L., Periman, E. (2023), “A QPO IN MKN 421 FROM ARCHIVAL RXTE DATA”, https://arxiv.org/abs/2305.07510

[28] Giustini, M., Miniutti, G., Saxton, R., (2020),”X-ray quasi-periodic eruptions from the galactic nucleus of RX J1301.9+2747”, https://arxiv.org/abs/2002.08967

[29] Pasham, D.R, et. al, (2024), “Alive but Barely Kicking: News from 3+ years of Swift and XMM-Newton X-ray Monitoring of Quasi-Periodic Eruptions from eRO-QPE1”, https://arxiv.org/abs/2402.09690

[30] Janiuk, A., et. Al., (2015),”Interplay between heartbeat oscillations and wind outflow in micro quasar IGR J17091-3624”, https://www.aanda.org/articles/aa/pdf/2015/02/aa25003-14.pdf

[31] Ingram, A., Motta, S., (2020), “A review of quasi-periodic oscillations from black hole X-ray binaries: observation and theory”, https://arxiv.org/abs/2001.08758

[32] Rom, R., (Apr 2023), “Matter Reactors”, Journal of High Energy Physics, Gravitation and Cosmology, 9, No. 2. https://www.scirp.org/journal/paperinformation.aspx?paperid=124154

[33] Corley, S., Jacobson, T., Black Hole Lasers (1999), https://arxiv.org/pdf/hep-th/9806203.pdf

[34] Daly, R., (2022), “Robust supermassive black hole spin mass-energy characteristics: a new method and results”, https://arxiv.org/abs/2210.07779

[35] Kaburaki, O. and Okamoto, I., (1991),”Kerr black holes as a Carnot engine”, Physical Review D 43(2):340-345, https://www.researchgate.net/publication/13276863_Kerr_black_holes_as_a_Carnot_engine

[36] Abramowicz, M. A., (2024), “Analytic models of accretion discs/3.1. Thin discs”, http://www.oa.uj.edu.pl/jets2011/talks/Abramowicz_talk_Krakow2011/001-Slides/Alternative/016-page.html

[37] Kozlowski, M., Jaroszynski, M., Abramowicz, M. A (2024), “The analytic theory of fluid disks orbiting the Kerr black hole”**,**

https://articles.adsabs.harvard.edu/pdf/1978A%26A....63..209K

[38] Abramowicz, M. A. et. al., (2010), “Leaving the innermost stable circular orbit: the inner edge of a black-hole accretion disc at various luminosities”,

https://www.arxiv.org/abs/1003.3887

[39] Abramowicz, M.A., Straub, O., (2014),”Accretion discs”,

http://www.scholarpedia.org/article/Accretion_discs

[40] Teukolsky, S. A., (2015), “The Kerr Metric”, https://arxiv.org/abs/1410.2130

[41] Mizuno, Y., (2022), “GRMHD Simulations and Modeling for Jet Formation and Acceleration Region in AGNs”, https://arxiv.org/pdf/2201.12608

[42] Siegel, E., (2024), “Does the Universe expand by stretching or creating space?”,

https://bigthink.com/starts-with-a-bang/universe-expand-stretching-creating-space/